JOC Article

# Evidence for Effective p(Z)−π(Ar) Conjugations (Z = S, Se, and Te, as Well as Z = O) in 9-(Arylchalcogenyl)triptycenes: Experimental and Theoretical Investigations

Satoko Hayashi,[†] Takashi Nakamoto,[†] Mao Minoura,[‡] and Waro Nakanishi*,[†]

*Department of Material Science and Chemistry, Faculty of Systems Engineering, Wakayama University, 930 Sakaedani, Wakayama 640-8510, Japan, and Department of Chemistry, School of Science, Kitasato University, Kitasato, Sagamihara, Kanagawa 228-8555, Japan*

*nakanisi@sys.wakayama-u.ac.jp*

*Received March 10, 2009*

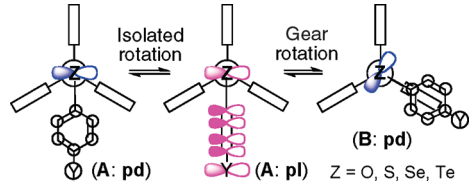


The p(Z)−π(Ar) conjugations must operate fully in the ground states of 9-(arylchalcogenyl)triptycenes (*p*-$YC_6H_4ZTpc$:**1** (Z = O), **2** (Z = S), **3** (Z = Se), and **4** (Z = Te)), where the *p*-$YC_6H_4$ group is placed in the bisected area between two phenyl planes of the triptycyl group with the parallel orientation. The ground-state geometries, which we call (**A**: **pl**), are confirmed by X-ray analysis. However, the conjugations never operate in the transition states between (**A**: **pl**) and/or the topomeric structures (**A′**: **pl′**), where the $Z-C_{Tpc}$ bond is perpendicular to the plane. The site-exchange processes correlate to the conjugations. Temperature-dependent $^1H$ NMR spectra are analyzed for **2** and **3** to demonstrate the effective p(Z)−π(Ar) conjugations. The activation energies for the interconversion between (**A**: **pl**) and (**A′**: **pl′**) (GR: gear process) were obtained for **2** ($\Delta G^{\ddagger}_{GR}$(**2**)) and **3** ($\Delta G^{\ddagger}_{GR}$(**3**)). $\Delta G^{\ddagger}_{GR}$(**3**) correlate well with $\Delta G^{\ddagger}_{GR}$(**2**), and $\Delta G^{\ddagger}_{GR}$(**2**) are well analyzed by the Hammett-type dual parameters. $\Delta G^{\ddagger}_{GR}$(**2**) and $\Delta G^{\ddagger}_{GR}$(**3**) are demonstrated to be controlled by the resonance interaction of the p(Z)−π($C_6H_4$)−p(Y) conjugations. QC calculations are performed on the ground and exited states of **1**−**4**, which clarify the effective p(Z)−π($C_6H_4$)−p(Y) conjugations for Z of heavier atoms.

## Introduction

Factors to control the fine structures of organic chalcogen compounds are of current interest.[1−16] The p(Z)−π($C_6H_4$)−p(Y) conjugation is applied to explain the fine structures of 1-(aryl-chalcogena)naphthalenes (1-(*p*-$YC_6H_4Z$)$C_{10}H_7$, 1-ArZNap (Z = O (**I**),[17] S (**II**),[17] Se (**III**),[17,18] and Te (**IV**);[17] Y = H (**a**), $NMe_2$ (**b**), OMe (**c**), Me (**d**), F (**e**), Cl (**f**), Br (**g**), COOEt (**h**), CN (**i**), and $NO_2$ (**j**)). Fine structures of **I**−**IV** are well explained by the p(Z)−π($C_6H_4$)−p(Y) conjugation. However, the contribution of the p(Z)−π(Ar) conjugation might not be accepted so easily, especially for Z of heavier elements, since the magnitudes of

* To whom correspondence should be addressed. Tel: +81 73 457 8252. Fax: +81 73 457 8253.
[†] Wakayama University.
[‡] Kitasato University.

(1) (a) *Molecular Interactions. From van der Waals to Strongly Bound Complexes*; Scheiner, S., Ed.; Wiley: New York, 1997. (b) Asmus, K. D. *Acc. Chem. Res.* **1979**, *12*, 436–442. (c) Musker, W. K. *Acc. Chem. Res.* **1980**, *13*, 200–206. (d) Kucsman, A.; Kapovits, I. Non-Bonded Sulfur-Oxygen Interaction in Organic Sulfur Compounds. In *Organic Sulfur Compounds in Organic Sulfur Chemistry: Theoretical and Experimental Advances*; Bernardi, F., Csizmadia, I. G., Mangini, A., Eds.; Elsevier: Amsterdam, 1985; Chapter 4.

(2) (a) *Chemistry of Hypervalent Compounds*; Akiba, K.-y., Ed.; Wiley-VCH: New York, 1999. (b) Nakanishi, W. Hypervalent Chalcogen Compounds. In *Handbook of Chalcogen Chemistry: New Perspectives in Sulfur, Selenium and Tellurium*; Devillanova, F. A., Ed.; Royal Society of Chemistry: Cambridge, 2006; Chapter 10.3, pp 644−668.

(3) Glusker, J. P. Directional aspects of intermolecular interactions. In *Topics in Current Chemistry, Design of Organic Solids*; Weber, E., Ed.; Springer Verlag: Berlin, Heidelberg, 1998; Vol. 198, pp 1−56.

(4) Iwaoka, M.; Tomoda, S. *J. Am. Chem. Soc.* **1996**, *118*, 8077–8084. Iwaoka, M.; Takemoto, S.; Tomoda, S. *J. Am. Chem. Soc.* **2002**, *124*, 10613–10620. Iwaoka, M.; Takemoto, S.; Okada, M.; Tomoda, S. *Chem. Lett.* **2001**, *30*, 132–133.

(5) (a) Nakanishi, W. *Chem. Lett.* **1993**, 2121–2122. (b) Nakanishi, W.; Hayashi, S.; Toyota, S. *Chem. Commun.* **1996**, 371–372. (c) Nakanishi, W.; Hayashi, S.; Yamaguchi, H. *Chem. Lett.* **1996**, 947–948. (d) Nakanishi, W.; Hayashi, S.; Toyota, S. *J. Org. Chem.* **1998**, *63*, 8790–8800. (e) Nakanishi, W.; Hayashi, S.; Uehara, T. *J. Phys. Chem. A* **1999**, *103*, 9906–9912. (f) Nakanishi, W.; Hayashi, S.; Arai, T. *Chem. Commun.* **2002**, 2416–2417. (g) Nakanishi, W.; Hayashi, S.; Morinaka, S.; Sasamori, T.; Tokitoh, N. *New J. Chem.* **2008**, *32*, 1881–1889.

10.1021/jo900488r CCC: $40.75 
Published on Web 06/08/2009

**CHART 1**

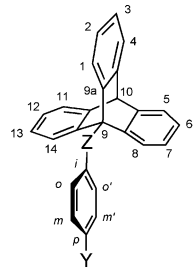

**1** (Z = O), **2** (Z = S), **3** (Z = Se), **4** (Z = Te), **5** (Z = $CH_2$)

| | a | b | b' | c | d | e | f | g | h | i | j |
|---|---|---|---|---|---|---|---|---|---|---|---|
| Y = | H | $NMe_2$ | $NH_2$ | OMe | Me | F | Cl | Br | COOEt | CN | $NO_2$ |

the p(Z)−$\pi$(Ar) conjugations are believed to decrease swiftly as Z becomes heavier. How can the magnitudes of the p(Z)−$\pi$(Ar) conjugation be elucidated? We searched for a suitable system that enables us to clarify the magnitudes of the p(Z)−$\pi$(Ar) conjugations.

9-(Arylchalcogenyl)triptycenes (*p*-$YC_6H_4$ZTpc (1-ArZTpc); Z = O (**1**),[19] S (**2**), Se (**3**),[20,21] and Te (**4**); Y = H (**a**), $NMe_2$ (**b**), OMe (**c**), Me (**d**), F (**e**), Cl (**f**), Br (**g**), COOEt (**h**), CN (**i**), and $NO_2$ (**j**)) are excellent candidates for that purpose (Chart 1). There are two conformers around the Z−$C_{Tpc}$ bond in **1**−**4**, **A** and **B**:[5c,6a−c,18,22] **A** corresponds to a conformer where the Z−$C_{Ar}$ bond is in the bisected area between two phenyl planes of the triptycyl group, and **B** corresponds to a conformer where the bond is on a phenyl plane of the triptycyl group. There are also two conformers around the Z−$C_{Ar}$ bond in **1**−**4**, **pl** and **pd**:[5c,d,6a,c,18,23] **pl** corresponds to a conformer where the Z−$C_{Tpc}$ bond is in the Ar plane and it is **pd** if the bond is perpendicular to the plane. Scheme 1 shows the (**A**: **pl**), (**A**: **pd**), and (**B**: **pd**) conformers, together with the interconversion process in **1**−**4**.[19−21] Isolated rotation (IR) may occur around the Z−$C_{Ar}$ bond, converting (**A**: **pl**) into (**A**: **pd**), and thence into the equivalent form (**A**: **pl′**) by further rotation of 180°, although (**A**: **pl′**) is not shown in Scheme 1. There are three equivalent conformations in **A**. Similarly, three conformers are in **B**. Interconversion between (**A**: **pl**) and (**A′**: **pl′**) may occur via (**B**: **pd**) where the primes imply the topomeric structures (Scheme 1). This process is referred to as gear rotation (GR).

**SCHEME 1. (A: pl), (A: pd), (B: pd), and (A′: pl′) Structures, Together with Interconversion, in 1−4**

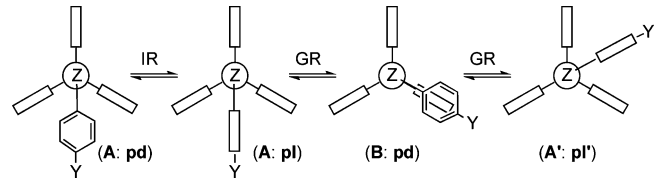


**SCHEME 2. p(Z)−$\pi$($C_6H_4$)−p(Y) (Z = O, S, Se, and Te) Conjugations in (A: pl), (A: pd), and (B: pd) for 1−4**

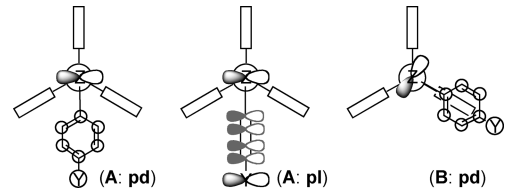


Very recently, some activation parameters were reported for the IR and GR processes in **3** by analyzing the temperature dependent $^1$H NMR spectra of **3a**, **3c**, **3i**, and **3j**, together with the results of quantum chemical (QC) calculations on **3a**, **3b′** (Y = $NH_2$), **3i**, and **3j**.[21] The activation parameters change depending on Y, although Y is limited. The results led us to believe that the magnitudes of the p(Z)−$\pi$($C_6H_4$)−p(Y) conjugation could be evaluated by analyzing the temperature dependent $^1$H NMR spectra of **1**−**4**. Scheme 2 illustrates the orbital interactions of the *p*-$YC_6H_4Z$ part in the triptycene systems **1**−**4**.

It is important to establish the (**A**: **pl**) structures of *p*-$YC_6H_4$ZTpc in the ground state to analyze the temperature-dependent $^1$H NMR spectra. The structures were determined for **1a**,**j**, **2a**,**j**, and 9-benzyltriptycene (**5a**)[19] by X-ray crystallographic analysis, in addition to **3a**−**c**,**f**,**j**.[21] The temperature-dependent $^1$H NMR spectra were measured and analyzed carefully to evaluate the magnitudes of the p(Z)−$\pi$($C_6H_4$)−p(Y) conjugation for **2** and **3** having various Y in $CD_2Cl_2$. The p(Z)−$\pi$($C_6H_4$)−p(Y) conjugation must operate fully in (**A**: **pl**), whereas the conjugation will not operate at all in (**A**: **pd**) and (**B**: **pd**). The activation processes for IR and GR must contain the loss of the p(Z)−$\pi$($C_6H_4$)−p(Y) conjugation. Quantum chemical (QC) calculations were also employed to analyze the

(6) (a) Nakanishi, W.; Hayashi, S.; Sakaue, A.; Ono, G.; Kawada, Y. *J. Am. Chem. Soc.* **1998**, *120*, 3635–3640. (b) Hayashi, S.; Nakanishi, W. *J. Org. Chem.* **1999**, *64*, 6688–6696. (c) Nakanishi, W.; Hayashi, S. *J. Org. Chem.* **2002**, *67*, 38–48. (d) Nakanishi, W.; Hayashi, S. *J. Organomett. Chem.* **2000**, *611*, 178–189. (e) Hayashi, S.; Nakanishi, W. *Bull. Chem. Soc. Jpn.* **2008**, *81*, 1605–1615. (f) Yamane, K.; Hayashi, S.; Nakanishi, W. *Polyhedron* **2008**, *27*, 3557–3566.

(7) (a) Hayashi, S.; Wada, H.; Ueno, T.; Nakanishi, W. *J. Org. Chem.* **2006**, *71*, 5574–5585. (b) Hayashi, S.; Nakanishi, W.; Furuta, A.; Drabowicz, J.; Sasamori, T.; Tokitoh, N. *New J. Chem.* **2009**, *33*, 196–206.

(8) (a) Nakanishi, W.; Hayashi, S.; Itoh, N. *Chem. Commun.* **2003**, 124–125. (b) Nakanishi, W.; Hayashi, S.; Itoh, N. *J. Org. Chem.* **2004**, *69*, 1676–1684. (c) Nakanishi, W.; Nakamoto, T.; Hayashi, S.; Sasamori, T.; Tokitoh, N. *Chem.—Eur. J.* **2007**, *13*, 255–268.

(9) Nakanishi, W.; Hayashi, S.; Yamaguchi, S.; Tamao, K. *Chem. Commun.* **2004**, 140–141.

(10) Nakanishi, W.; Hayashi, S.; Narahara, K. *J. Phys. Chem. A* **2008**, *112*, 13593–13599.

(11) Rosenfield, R. E.; Parthasarathy, R., Jr.; Dunitz, J. D. *J. Am. Chem. Soc.* **1977**, *99*, 4860–4862.

(12) *The Weak Hydrogen Bond in Structural Chemistry and Biology; International Union of Crystallography Monographs on Crystallography*; Desiraju, G. R., Steiner, T., Eds.; Oxford University Press: New York, 1999. *Crystal Design: Structure and Function (Perspectives in Supramolecular Chemistry)*; Desiraju, G. R., Ed.; John Wiley & Sons: New York, 2003; Vol. 6.

(13) Steiner, T. *Angew. Chem.* **2002**, *114*, 50–80. *Angew. Chem., Int. Ed.* **2002**, *41*, 48−76.

(14) Bleiholder, C.; Werz, D. B.; Köppel, H.; Gleiter, R. *J. Am. Chem. Soc.* **2006**, *128*, 2666–2674. Bleiholder, C.; Gleiter, R.; Werz, D. B.; Köppel, H. *Inorg. Chem.* **2007**, *46*, 2249–2260.

(15) Rêthorê, C.; Madalan, A.; Fourmigué, M.; Canadell, E.; Lopes, E. B.; Almeida, M.; Clêrac, R.; Avarvari, N. *New J. Chem.* **2007**, *31*, 1468–1483.

(16) Werz, D. B.; Gleiter, R.; Rominger, F. *J. Am. Chem. Soc.* **2002**, *124*, 10638–10639. (a) Gleiter, R.; Werz, D. B.; Rausch, B. J. *Chem.—Eur. J.* **2003**, *9*, 2676–2683. (b) Werz, D. B.; Gleiter, R.; Rominger, F. *J. Org. Chem.* **2004**, *69*, 2945–2952. (c) Gleiter, R.; Werz, D. B. *Chem. Lett.* **2005**, *34*, 126–131. (d) Werz, D. B.; Rausch, B. J.; Gleiter, R. *Tetrahedron Lett.* **2002**, *43*, 5767–5769.

(17) Nakai, T.; Hayashi, S.; Nakanishi, W. *Phosphorus, Sulfur, Silicon Relat. Elem.* **2009**, in press.

(18) (a) Nakanishi, W.; Hayashi, S.; Uehara, T. *Eur. J. Org. Chem.* **2001**, 3933–3943. (b) Yamane, K.; Hayashi, S.; Nakanishi, W. *J. Org. Chem.* **2007**, *72*, 7587–7596.

(19) For **1a** and **5a**: Yamamoto, G. *Tetrahedron* **1990**, *46*, 2761–2772.

(20) Nakamoto, T.; Hayashi, S.; Nakanishi, W. *J. Org. Chem.* **2008**, *73*, 9259–9269.

(21) Nakamoto, T.; Hayashi, S.; Nakanishi, W.; Minoura, M.; Yamamoto, G. *New J. Chem.* **2009**, in press ( DOI: 10.1039/b817949b).

(22) Nakanishi, W.; Hayashi, S.; Uehara, T. *J. Phys. Chem. A* **1999**, *103*, 9906–9912.

(23) Nakanishi, W.; Hayashi, S.; Shimizu, D.; Hada, M. *Chem.—Eur. J.* **2006**, *12*, 3829–3846.

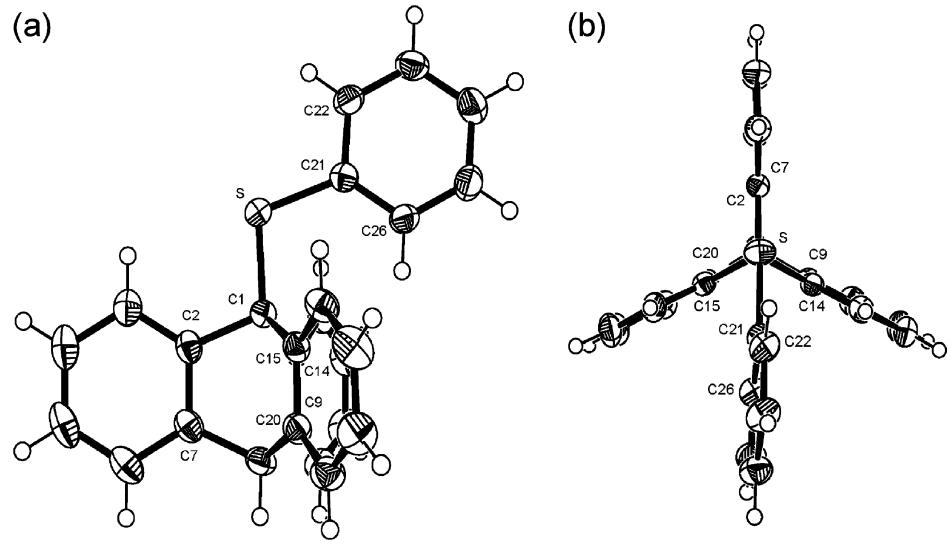


**FIGURE 1.** ORTEP drawing of **2a** with atomic numbering scheme for selected atoms (50% probability thermal level): (a) side view and (b) top view.

process and to evaluate the magnitudes of the p(Z)−$\pi$($C_6H_4$)−p(Y) conjugation containing Z of heavier elements.

Here, we discuss the p(Z)−$\pi$($C_6H_4$)−p(Y) conjugation through the activation energies in $^1$H DNMR spectra of **2** and **3**, after the establishment of the (**A**: **pl**) structures by the X-ray crystallographic analysis for the ground states. QC calculations were performed on **1**−**4** with Y = H (**a**), $NH_2$ (**b′**), and $NO_2$ (**j**) to evaluate the magnitudes of the p(Z)−$\pi$($C_6H_4$)−p(Y) (Z = O, S, Se, and Te) conjugation, together with 9-(arylmethyl)triptycenes (**5**: *p*-$YC_6H_4CH_2$Tpc)[19] for convenience of comparison.

## Results and Discussion

**Structure of 9-(*p*-$YC_6H_4$ZTpc).** The X-ray crystallographic analysis was carried out for suitable single crystals of **1a**,**j**, **2a**,**j**, and **5a**. Only one type of structure corresponds to each of them in the crystals. Figure 1 shows the structure of **2a**. Those of **1a**, **1j**, **2j**, and **5a** are shown in the Supporting Information (Figures S1−S4, respectively). The structures of **3a**−**c**,**f**,**j** are shown in a previous paper.[21] The selected interatomic distances, angles, and torsional angles of **1a**,**j**, **2a**,**j**, and **5a**, together with **3a**,[21] necessary for the discussion, are collected in Table S1 of the Supporting Information.

The structures of **1a**,**j**, **2a**,**j**, and **5a** are all (**A**: **pl**) in crystals: The torsional angles of C21ZC1C2 ($\phi$(C21ZC1C2)) are close to 180° (or −180°), and the magnitudes of $\phi$(C1ZC21C26) are less than ca. 10°. The structures are close to the $C_s$ symmetry. The crystal packing effect must be mainly responsible for the deviations. The steric compression seems small for these compounds. The results strongly support that (**A**: **pl**) is the ground-state structure for **1**−**5**.

After confirmation of the (**A**: **pl**) structure for **1**−**3** and **5** in the ground state, next extension is to clarify the p(Z)−$\pi$(Ar) conjugations through the dynamic stereochemistry employing **2** and **3**.

**Dynamic NMR Spectroscopy.** Temperature-dependent $^1$H NMR spectra were measured for **2a**−**j** at various temperatures in $CD_2Cl_2$ using a 400 MHz NMR spectrometer. Similar spectra were also measured for **3a**−**j** at 400 MHz although the spectra were already reported for **3a**,**c**,**i**,**j** measured at 600 MHz.[21,24] Figure 2 shows the spectra for **2j** measured at 400 MHz, for example. Figure 2 also contains the calculated line-shape change[25] of the aromatic protons for the GR process in the triptycyl group for **2j**. The spectra of the calculated line-shape change[25] of the aromatic protons for the IR process in the *p*-nitrophenyl group for **2j** are shown in Figure S5 of the Supporting Information. The spectra for **2a**−**i** and **3a**−**j** are shown in Figures S6−S26 of the Supporting Information.

The Gibbs free energies of activation ($\Delta G^{\ddagger}$) were evaluated for GR in **2i** and **2j** based on the line-shape analysis.[25] The $\Delta G^{\ddagger}$ values are 44.0 and 45.0 kJ mol$^{-1}$, respectively, at −60 °C. The temperature dependence of $\Delta G^{\ddagger}$ will give the $\Delta H^{\ddagger}$ and $\Delta S^{\ddagger}$ values by plotting $\Delta G^{\ddagger}$ versus $T^{-1}$ in K$^{-1}$. The ($\Delta H^{\ddagger}$, $\Delta S^{\ddagger}$) values are evaluated to be (42.8 kJ mol$^{-1}$, −5.7 J mol$^{-1}$) and (41.2 kJ mol$^{-1}$, −17.4 J mol$^{-1}$) for **2i** and **2j**, respectively. Similarly, the ($\Delta G^{\ddagger}$, $\Delta H^{\ddagger}$, $\Delta S^{\ddagger}$) values for IR at −60 °C are evaluated to be (39.0 kJ mol$^{-1}$, 35.3 kJ mol$^{-1}$, −17.8 J mol$^{-1}$) and (40.8 kJ mol$^{-1}$, 32.4 kJ mol$^{-1}$, −39.6 J mol$^{-1}$) for **2i** and **2j**, respectively. The ($\Delta G^{\ddagger}$, $\Delta H^{\ddagger}$, $\Delta S^{\ddagger}$) values for GR in **3i** and **3j** at −60 °C are also evaluated to be (41.4 kJ mol$^{-1}$, 36.9 kJ mol$^{-1}$, −22.4 J mol$^{-1}$) and (41.8 kJ mol$^{-1}$, 34.3 kJ mol$^{-1}$, −37.1 J mol$^{-1}$), respectively. The negative values of $\Delta S^{\ddagger}$ may show that the rotational freedom around the bond in question becomes tighter in the transition state relative to that in the ground state. Table 1 collects the results for **2f**−**j** and **3g**−**j** similarly evaluated by the line-shape analysis.

The coalescence method was also employed to evaluate the activation energies of **2** and **3**, since the complete line-shape analysis was difficult to apply to the spectra for **2a**−**e** and **3a**−**f**:

(24) Temperature-dependent $^1$H NMR spectra should also be measured for the tellurium compounds **4a**−**j** at various temperatures for better understanding of the p(Te)−$\pi$($C_6H_4$)−p(Y) conjugation. The activation energies for the GR and IR processes of **4a** are predicted to be 30 and 13 kJ mol$^{-1}$, respectively (see Table 3 and Figure 5). The values are smaller than those for **2a** by 5 and 20 kJ mol$^{-1}$, respectively. The results may show that it is difficult to obtain suitable temperature-dependent $^1$H NMR spectra of **4a**−**j** that evaluate reliable activation energies under our experimental conditions with a 400 MHz $^1$H NMR spectrometer. Nevertheless, we are interested in the $^{125}$Te NMR chemical shifts of **4a**−**j**, since they could be the standard of $\delta$(Te) for the planar structures of *p*-$YC_6H_4$TeR.

(25) Budzelaar, P. H. M. *gNMR*, version 5.0.6.0; Ivorysoft: Nijmegen, The Netherlands, 2006.

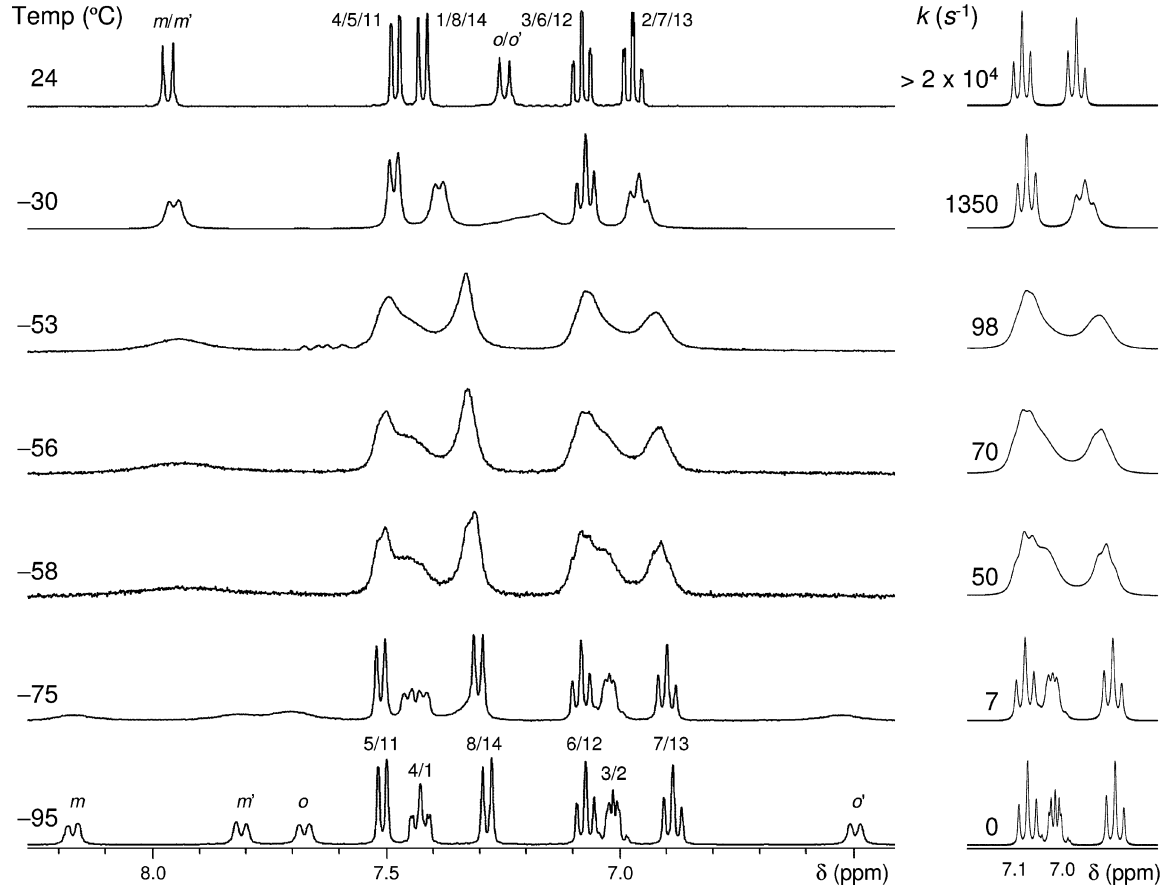


**FIGURE 2.** Observed $^1$H NMR spectra due to the aromatic proton region of **2j** in $CD_2Cl_2$ at various temperatures (a) and the calculated spectra with the best-fit rate constants for the aromatic protons of the triptycyl group for the GR process (b).

**TABLE 1.** $\Delta G^{\ddagger}$ (−60 °C)$\Delta H^{\ddagger}$, $\Delta S^{\ddagger}$ Values of the GR and IR Processes in 2f−j and 3g−j[a,b]

| compd | rot. | position[c] | $k$ (−60 °C) (s$^{-1}$) | $\Delta G^{\ddagger}$ (−60 °C) (kJ mol$^{-1}$) | $\Delta H^{\ddagger}$ (kJ mol$^{-1}$) | $\Delta S^{\ddagger}$ (J mol$^{-1}$) | $r$[d] | temp range (°C) | $n$[e] |
|---|---|---|---|---|---|---|---|---|---|
| **2f** | GR | 3/6/12 | 92.4 | 38.75 | 32.08 | −35.10 | −0.999 | −95 to −60 | 7 |
| **2g** | GR | 3/6/12 | 83.6 | 39.34 | 35.43 | −20.39 | −0.999 | −95 to −60 | 8 |
| **2h** | GR | 3/6/12 | 79.2 | 42.55 | 38.40 | −20.03 | −0.999 | −85 to −50 | 11 |
| **2h** | IR | *m*/*m*′ | 437 | 37.81 | 32.99 | −24.51 | −0.999 | −95 to −30 | 6 |
| **2i** | GR | 3/6/12 | 73.7 | 44.00 | 42.79 | −5.69 | −0.999 | −75 to −48 | 10 |
| **2i** | IR | *m*/*m*′ | 712 | 38.96 | 35.27 | −17.77 | −1.000 | −95 to −15 | 9 |
| **2j** | GR | 3/6/12 | 68.6 | 44.95 | 41.18 | −17.36 | −1.000 | −75 to −42 | 9 |
| **2j** | IR | *m*/*m*′ | 319 | 40.76 | 32.44 | −39.63 | −0.998 | −90 to −30 | 10 |
| **3g** | GR | 3/6/12 | 69.7 | 37.99 | 36.88 | −5.99 | −0.997 | −95 to −75 | 7 |
| **3h** | GR | 3/6/12 | 73.2 | 40.28 | 39.24 | −5.32 | −0.998 | −80 to −55 | 9 |
| **3i** | GR | 3/6/12 | 70.2 | 41.40 | 36.90 | −22.40 | −0.998 | −80 to −60 | 9 |
| **3j** | GR | 3/6/12 | 72.4 | 41.84 | 34.31 | −37.09 | −0.998 | −80 to −55 | 10 |

[a] Measured in $CD_2Cl_2$. [b] Determined by line-shape analysis. [c] See Chart 1. [d] Correlation coefficient. [e] Sampling number for the analysis.

the separation of the signals necessary for the analysis was incomplete at the lowest temperature that can be achieved under our measurement conditions. The activation energies for GR, corresponding to the process from**2** (**A**: **pl**) to **2** (**B**: **pd**), were evaluated by the coalescence method (see eq 5).[26] Table 2 summarizes the activation energies of **2** and **3** for GR, although those of **2b**,**c**,**e**, and **3a**−**e** are given as the upper limit in the experiment. Table 2 also contains the values for IR in **2h**−**j**, together with those for GR and IR of **1a**[19] and **5a**[19] reported in the literature.

The activation energies for GR in **2** and **3** were determined. The behaviors of those parameters are examined next.

**Behaviors of $\Delta G^{\ddagger}_{GR}$(2) and $\Delta G^{\ddagger}_{GR}$(3).** How do $\Delta G^{\ddagger}_{GR}$(**3**) correlate to $\Delta G^{\ddagger}_{GR}$(**2**)? $\Delta G^{\ddagger}_{GR}$(**3**) are plotted versus $\Delta G^{\ddagger}_{GR}$(**2**). Figure 3 shows the results. The solid circle stands for the reasonably determined values, whereas the hollow circle does the upper limit in the experiments. The correlation is good ($r$ = 0.997) for the solid circle of Y = Cl, Br, COOEt, CN, and $NO_2$ in Figure 3. The data for Y = $NMe_2$, OMe, and F in both **2** and **3** and for Y = Me and H in **3** correspond to the upper limit in the measurements. The activation energies for GR in **2** correlate very well to those in **3**. The results must show that a simple and common mechanism is operating in the GR process both in **2** and **3**. The larger $\Delta G^{\ddagger}_{GR}$(**2**) relative to $\Delta G^{\ddagger}_{GR}$(**3**) would be the reflection of the shorter S−C bonds in **2** relative to the Se−C bonds in **3**, which must lead the higher energy transition state for **2** relative to that for **3**.

It must be of interest if the experimental $\Delta G^{\ddagger}_{GR}$(**2**) values are correlated to other energy parameters. The $\Delta G^{\ddagger}_{GR}$ values for **2a** (Y = H), **2e** (Y = F), **2f** (Y = Cl), and **2g** (Y = Br) are

**TABLE 2. Rate Constants and Free Energies of Activation of the GR and/or IR Processes in 1−5**

| compd | Z | Y | $k_{GR}$[a](s$^{-1}$) | $\Delta G^{\ddagger}_{GR}$[a](kJ mol$^{-1}$) | $\Delta G^{\ddagger}_{GR}$[b] (kJ mol$^{-1}$) | $T_c$ (°C) | process |
|---|---|---|---|---|---|---|---|
| **2b** | S | $NMe_2$ | | *d* | <36.9 | <−95 | GR |
| **2c** | S | OMe | | *d* | <36.9 | <−95 | GR |
| **2d** | S | Me | | *d* | 37.2 | −94 | GR |
| **2a** | S | H | | *d* | 37.8 | −91 | GR |
| **2e** | S | F | | *d* | <36.9 | <−95 | GR |
| **2f** | S | Cl | 92.4 | 38.75 | 39.1 | −83 | GR |
| **2g** | S | Br | 83.6 | 39.34 | 39.8 | −81 | GR |
| **2h** | S | $CO_2Et$ | 79.2 | 42.55 | 42.8 | −66 | GR |
| **2i** | S | CN | 73.7 | 44.00 | 44.5 | −60 | GR |
| **2j** | S | $NO_2$ | 68.6 | 44.95 | 45.4 | −56 | GR |
| **2h** | S | $CO_2Et$ | 437 | 37.81 | | −75 | IR |
| **2i** | S | CN | 712 | 38.96 | | −65 | IR |
| **2j** | S | $NO_2$ | 319 | 40.76 | | −63 | IR |
| **3b** | Se | $NMe_2$ | | *d* | <36.9 | <−95 | GR |
| **3c** | Se | OMe | | *d* | <36.9 | <−95 | GR |
| **3d** | Se | Me | | *d* | <36.9 | <−95 | GR |
| **3a** | Se | H | | *d* | <36.9 | <−95 | GR |
| **3e** | Se | F | | *d* | <36.9 | <−95 | GR |
| **3f** | Se | Cl | | *d* | 37.5 | −93 | GR |
| **3g** | Se | Br | 69.7 | 37.99 | 38.1 | −88 | GR |
| **3h** | Se | $CO_2Et$ | 73.2 | 40.28 | 40.7 | −78 | GR |
| **3i** | Se | CN | 70.2 | 41.40 | 41.6 | −72 | GR |
| **3j** | Se | $NO_2$ | 72.4 | 41.84 | 42.5 | −70 | GR |
| **1a**[d] | O | H | $10^5$ | ≈ 29 | | | GR |
| **1a**[d] | O | H | $10^2$ | ≈ 62 | | | IR |
| **5a**[d] | $CH_2$ | H | 52 | 44.8 | | | GR |
| **5a**[d] | $CH_2$ | H | 2350 | 38.1 | | | IR |

[a] Obtained by line-shape analysis of $^1$H DNMR spectra at −60 °C. [b] Calculated from the coalescence temperature. [c] Coalescence temperature. [d] Ref 19.

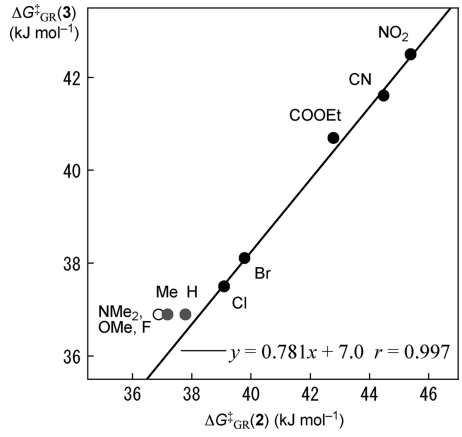


**FIGURE 3.** Plot of $\Delta G^{\ddagger}_{GR}$(**3**) vs $\Delta G^{\ddagger}_{GR}$(**2**).

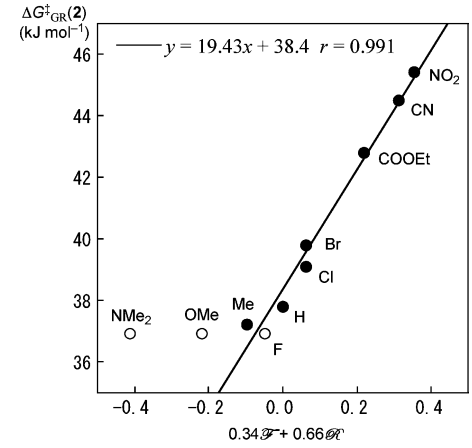


**FIGURE 4.** Plot of $\Delta G^{\ddagger}_{GR}$(**2**) vs $0.34\mathcal{F} + 0.66\mathcal{R}$.

37.8, less than 37, 39.1, and 39.8 kJ mol$^{-1}$, respectively. The value for **2e** is evaluated to be smaller than those of **2a**,**f**, and **2g**, which must be the reflection of the substantial donating ability of *F* in $\Delta G^{\ddagger}_{GR}$(**2**) through the resonance mechanism operating in (**A**: **pl**): the mechanism will disappear in the transition states for GR of (**B**: **pd**). Therefore, $\Delta G^{\ddagger}_{GR}$(**2**) are expected to be well understood by the Hammett-type dual parameter analysis.

The Swain−Lupton's $\mathcal{F}$ and $\mathcal{R}$ parameters are employed for the plots.[27] Figure 4 shows the plot of $\Delta G^{\ddagger}_{GR}$(**2**) versus $0.34\mathcal{F} + 0.66\mathcal{R}$. The correlation is good ($r = 0.991$), which is given in Figure 4. The results demonstrate that $\Delta G^{\ddagger}_{GR}$(**2**) are well correlated to the energy parameters exemplified by $\mathcal{F}$ and $\mathcal{R}$: Other parameters could be used similarly, since the Hammett-type parameters are correlated closely with each other. The results demonstrate that the resonance mechanism is predominantly operating in the p(S)−π(Ar) conjugation in **2** (**A**: **pl**). Similar resonance mechanism of the p(Se)−π(Ar) conjugation must also operate in **3** (**A**: **pl**), judging from the correlation between **3** (**A**: **pl**) and **2** (**A**: **pl**) shown in Figure 3. The mechanism can be described by the p(Z)−π($C_6H_4$)−p(Y) conjugation.

The role of the p(Z)−π($C_6H_4$)−p(Y) conjugation to stabilize the conformers is established for **2** (Z = S) and **3** (Z = Se). Next extension is to clarify whether the conjugation is operating in **4** (Z = Te) or not. QC calculations are performed on (**A**: **pl**), (**A**: **pd**), and (**B**: **pd**) for **1**−**5** with Y = H (**a**), $NH_2$ (**1b′**), and $NO_2$ (**j**). The results will elucidate the energy profiles in **1**−**5** in the IR and/or GR processes.

**Energy Profiles of 1−5 Elucidated by QC Calculations.** QC calculations were performed on **1**−**5** with Y = H (**a**), $NH_2$

(26) Pople, J. A.; Schneider, W. G.; Bernstein, H. J. *High-resolution Nuclear Magnetic Resonance*; McGraw-Hill: New York, 1959; 218−224.
(27) Swain, C. G.; Lupton, E. C. *J. Am. Chem. Soc.* **1968**, *90*, 4328–4337.

**TABLE 3. Energies for 1−5 with Y = H (a), $NH_2$ (b′), and $NO_2$ (j), Calculated at the MP2 Level**[a]

| Y | | $NH_2$ (**b′**) | H (**a**) | $NO_2$ (**j**) |
|---|---|---|---|---|
| **1** (Z = O) | | | | |
| $E$ (**A**: **pl**)[b–d] | | −1128.6087 | −1073.4200 | −1277.5190 |
| $\Delta E$ (TS: GR) [e,f] | $E_{A:\,pd} - E_{A:\,pl}$ | 23.6 | 27.5 | 33.4 |
| $\Delta\Delta E$ (TS: GR) [e,g] | $\Delta E_{Y=Y} - \Delta E_{Y=H}$ | −3.9 | 0.0 | 5.9 |
| $\Delta E$ (TS: IR) [e,f] | $E_{B:\,pd} - E_{A:\,pl}$ | 56.2 | 60.0 | 65.4 |
| $\Delta\Delta E$ (TS: IR) [e,g] | $\Delta E_{Y=Y} - \Delta E_{Y=H}$ | −3.8 | 0.0 | 5.4 |
| **2** (Z = S) | | | | |
| $E$ (**A**: **pl**)[b–d] | | −1451.2093 | −1396.0191 | −1600.0223 |
| $\Delta E$ (TS: GR) [e,f] | $E_{B:\,pd} - E_{A:\,pl}$ | 29.6 | 35.0 | 41.5 |
| $\Delta\Delta E$ (TS: GR) [e,g] | $\Delta E_{Y=Y} - \Delta E_{Y=H}$ | −5.4 | 0.0 | 6.5 |
| $\Delta E$ (TS: IR) [e,f] | $E_{A:\,pd} - E_{A:\,pl}$ | 28.7 | 34.1 | 39.6 |
| $\Delta\Delta E$ (TS: IR) [e,g] | $\Delta E_{Y=Y} - \Delta E_{Y=H}$ | −5.4 | 0.0 | 5.5 |
| **3** (Z = Se) | | | | |
| $E$ (**A**: **pl**)[b,d] | | −3453.6003 | −3398.4101 | −3602.4129 |
| $\Delta E$ (TS: GR) [e,f] | $E_{B:\,pd} - E_{A:\,pl}$ | 29.0 | 34.0 | 39.9 |
| $\Delta\Delta E$ (TS: GR) [e,g] | $\Delta E_{Y=Y} - \Delta E_{Y=H}$ | −5.0 | 0.0 | 5.9 |
| $\Delta E$ (TS: IR) [e,f] | $E_{A:\,pd} - E_{A:\,pl}$ | 20.4 | 25.1 | 30.0 |
| $\Delta\Delta E$ (TS: IR) [e,g] | $\Delta E_{Y=Y} - \Delta E_{Y=H}$ | −4.7 | 0.0 | 4.9 |
| **4** (Z = Te) | | | | |
| $E$ (**A**: **pl**)[b–d] | | −7665.4177 | −7610.2266 | −7814.2288 |
| $\Delta E$ (TS: GR) [e,f] | $E_{B:\,pd} - E_{A:\,pl}$ | 26.3 | 30.3 | 35.9 |
| $\Delta\Delta E$ (TS: GR) [e,g] | $\Delta E_{Y=Y} - \Delta E_{Y=H}$ | −4.0 | 0.0 | 5.6 |
| $\Delta E$ (TS: IR) [e,f] | $E_{A:\,pd} - E_{A:\,pl}$ | 10.2 | 13.8 | 18.2 |
| $\Delta\Delta E$ (TS: IR) [e,g] | $\Delta E_{Y=Y} - \Delta E_{Y=H}$ | −3.5 | 0.0 | 4.4 |
| **5** (Z = $CH_2$) | | | | |
| $E$ (**A**: **pl**)[b–d] | | −1092.7077 | −1037.5206 | −1241.5239 |
| $\Delta E$ (TS: GR) [e,f] | $E_{B:\,pd} - E_{A:\,pl}$ | 49.2 | 50.0 | 52.6 |
| $\Delta\Delta E$ (TS: GR) [e,g] | $\Delta E_{Y=Y} - \Delta E_{Y=H}$ | −0.8 | 0.0 | 2.6 |
| $\Delta E$ (TS: IR) [e,f] | $E_{A:\,pd} - E_{A:\,pl}$ | 41.5 | 43.2 | 46.1 |
| $\Delta\Delta E$ (TS: IR) [e,g] | $\Delta E_{Y=Y} - \Delta E_{Y=H}$ | −1.7 | 0.0 | 2.9 |

[a] The 6-31G(d) basis sets were employed for H, C, and N in **1**−**5** and O in **2**−**5**. The 6-311+G(d,p) basis sets were for O in **1**, S in **2**, and Se in **3**, and the reported basis sets of the (7433111/743111/7411/2 + 1s1p1d1f) type were for for Te in **4** (see ref 30). [b] Global minimum. [c] In au. [d] Taken as the standard. [e] In kJ $mol^{-1}$. [f] Relative to (**A**: **pl**). [g] Relative to Y = H (**a**).

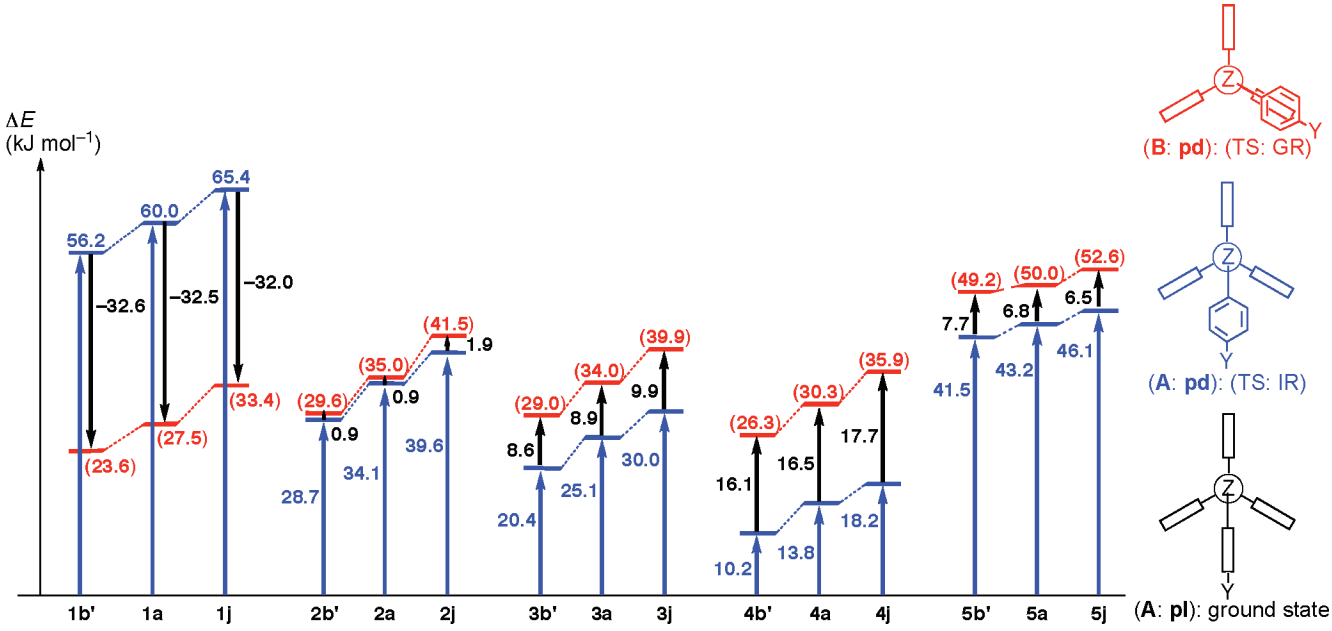


**FIGURE 5.** Predicted energy differences between (**A**: **pd**), (**A**: **pl**), and (**B**: **pd**) for **1**−**5**.

(**1b′**), and $NO_2$ (**j**) using the Gaussian 03 program.[28] The Møller−Plesset second-order energy correlation (MP2)[29] level was applied for the calculations. The 6-31G(d) basis sets were employed for H, C, and N of **1**−**5**. The 6-311+G(d) basis sets were employed for O in **1**, whereas the 6-31G(d) basis sets for O in **2**−**5**. The 6-311+G(d) basis sets were employed for S and Se in **2** and **3** and the reported basis sets[30] of the (7433111/

(28) Frisch, M. J. et al. *Gaussian 03, Revision D.02*; Gaussian, Inc.: Wallingford, CT, 2004.

(29) Møller, C.; Plesset, M. S. *Phys. Rev.* **1934**, *46*, 618–622. Gauss, J. *J. Chem. Phys.* **1993**, *99*, 3629–3643. Gauss, J. *Ber. Bunsen Ges.* **1995**, *99*, 1001–1008.

(30) Koga, T.; Yamamoto, S.; Shimazaki, T.; Tatewaki, H. *Theor. Chem. Acc.* **2002**, *108*, 41–45. Sekiya, M.; Noro, T.; Osanai, Y.; Koga, T. *Theor. Chem. Acc.* **2001**, *106*, 297–300.

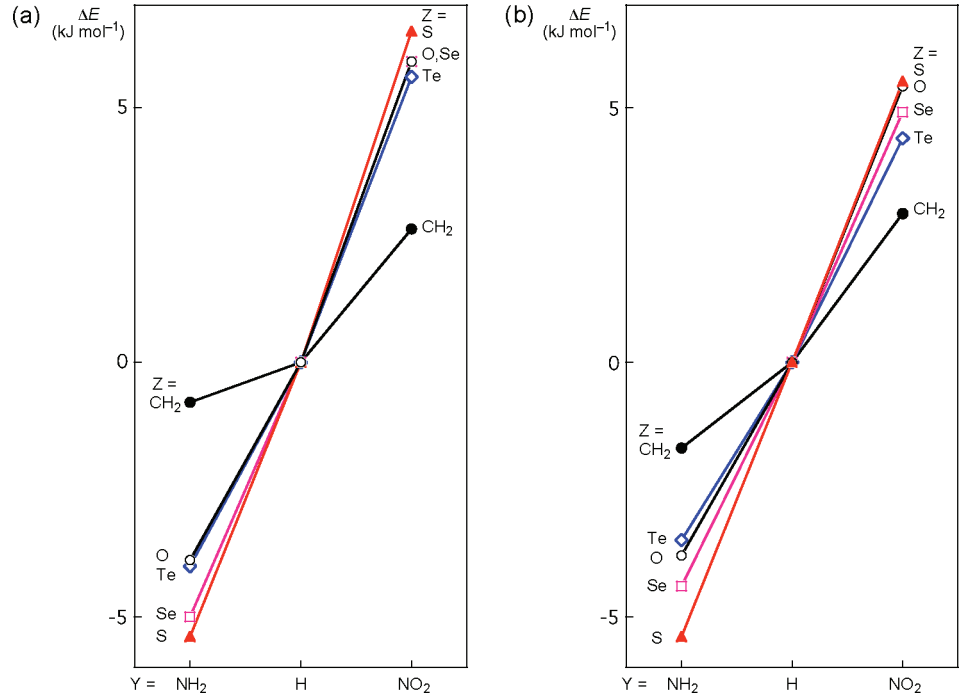


**FIGURE 6.** Calculated activation energies for Y = $NH_2$ and $NO_2$ relative to Y = H: in GR (a) and IR (b).

743111/7411/2 + 1s1p1d1f) type for Te in **4**. Table 3 collects the energies of (**A**: **pl**), (**A**: **pd**), and (**B**: **pd**) for **1**−**5** with Y = H (**a**), $NH_2$ (**1b′**), and $NO_2$ (**j**).

As shown in Table 3, the (**A**: **pl**) structure is optimized as the global minima for all of **1**−**5** at the MP2 level. As discussed in our previous paper,[21] (**B**: **pd**) can be identified as the transition state for the GR process and (**A**: **pd**) can be that for the IR process in **1**−**5**.[31] Figure 5 predicts the energy differences between (**A**: **pd**), (**A**: **pl**), and (**B**: **pd**) for **1**−**5**. The activation energy for GR is predicted to be larger than the corresponding IR for **2**−**5**. The observed energies of the GR and IR processes in **5a** are reported to be 44.8 and 38.1 kJ $mol^{-1}$, respectively,[19] whereas the activation energies for the GR and IR processes are predicted to be 50.0 and 43.2 kJ $mol^{-1}$ for **5a**, respectively. The calculated activation energies for the GR and IR processes are ca. 5 kJ $mol^{-1}$ larger than those of observed ones. The observed activation energies for GR is 6.7 kJ $mol^{-1}$ larger than that for IR in **5a**.[32] The difference between the two processes is predicted to be 6.8 kJ $mol^{-1}$, which reproduces well the observed difference.

On the other hand, the activation energy for the GR process is predicted to be smaller than the IR energy for **1** (Z = O). The very rough values are reported based on the temperature-dependent $^1$H NMR signals of **1a**, which are 29 and 62 kJ $mol^{-1}$, respectively.[19] The activation energies for the GR and IR processes in **1a** are predicted to be 28 and 60 kJ $mol^{-1}$, respectively. The calculated values are very close to the observed ones. For **2** (Z = S), almost equal activation energies are predicted for GR and IR. The energies for GR and IR are predicted to be 41.5 and 39.6 kJ $mol^{-1}$ for **2j**, respectively. However, the observed values are 45.0 and 40.8 kJ $mol^{-1}$, respectively, for **2j**. While the activation energy for IR is reproduced well by the calculations, that for GR seems larger by the calculations. In the case **3** (Z = Se), the activation energy for the IR process is predicted to be smaller than that of the GR process. The observed values for the GR process are <37 and 41.8 kJ $mol^{-1}$ for **3a** and **3j**, respectively.[21] The values are predicted to be 34.0 and 39.9 kJ $mol^{-1}$, respectively. The predicted values well reproduce the observed values, although the thermal effect is not considered. While temperature dependent $^1$H NMR spectra were not measured for **4** (Z = Te), the activation energies for the GR and IR processes are calculated at the MP2 level.[24] The activation energies predicted for IR are much smaller than the corresponding values for GR: The differences amount to 16−18 kJ $mol^{-1}$. Nevertheless, (**A**: **pd**) is predicted to be more stable than (**A**: **pl**) by 10.2 kJ $mol^{-1}$ at the MP2 level for **4b′** (Y = $NH_2$), which support that (**A**: **pl**) is the global minimum of **4**.

Figure 6 shows the plots of the activation energies of Y = $NH_2$ and $NO_2$ relative to Y = H in GR and IR for **1**−**5**. Equations 1−4 summarize the relative values of the activation energies shown in Figure 6. The orders are as follows.

$$Z = CH_2\ (-0.8\ kJ\ mol^{-1}) \gg O\ (-3.9) \geq Te\ (-4.0) > Se\ (-5.0) > S\ (-5.4)\ for\ Y = NH_2\ in\ GR \quad (1)$$

$$Z = CH_2\ (2.6kJ\ mol^{-1}) \ll Te\ (5.6) < O\ (5.9) = Se\ (5.9) < S\ (6.5)\ for\ Y = NO_2\ in\ GR \quad (2)$$

$$Z = CH_2\ (-1.7kJ\ mol^{-1}) \gg Te\ (-3.5) > O\ (-3.8) > Se\ (-4.7) > S\ (-5.4)\ for\ Y = NH_2\ in\ IR \quad (3)$$

$$Z = CH_2\ (2.9kJ\ mol^{-1}) \ll Te\ (4.4) < Se\ (4.9) < O\ (5.4) \leq S\ (5.5)\ for\ Y = NO_2\ in\ IR \quad (4)$$

Equations 1 and 2 correspond to panel a of Figure 6 (GR) and eqs 3 and 4 to panel b of Figure 6 (IR). The molecular orbital interactions of the p(Z)−π($C_6H_4$)−p(Y) conjugation illustrated in Scheme 2 helps us to understand the energy profiles of **1**−**4**. The positive stabilizing effect in the p(Z)−π($C_6H_4$)−p(Y) conjugations by Y = $NO_2$ must be the reflection of the energy lowering effect by the group at the ground state

geometries relative to TS, where the effect by Y = H is taken as the standard for each ($\Delta\Delta E$). On the other hand, the negative values in $\Delta\Delta E$ by Y = $NH_2$ must be due to the destabilizing effect in the conjugations at the ground states. The destabilizing effect of the p(Z)−$\pi$($C_6H_4$)−p(Y) conjugations by Y = $NH_2$ occurs in the ground state due to the strong donating ability for both Z and Y, which disappears in TS.

As shown in panel a of Figure 6 and eqs 1 and 2 for the GR process, the magnitude of the destabilizing effect in the p(Z)−$\pi$($C_6H_4$)−p(Y) conjugations by Y = $NH_2$ at the ground states becomes larger in the order Z = $CH_2$ ≪ O ≤ Te < Se < S. On the other hand, that of the stabilizing effect by Y = $NO_2$ at the ground states is in the order Z = $CH_2$ ≪ Te < O = Se < S. The order is commonly described as Z = $CH_2$ ≪ Te < Se < S with the changeable position of O, (very) close to Te. The results strongly suggest that the p(Z)−$\pi$($C_6H_4$)−p(Y) conjugations operate effectively for Z = S, Se, and Te, as well as O, although the inductive effect must also operate to affect the system in addition to the conjugations. Similar trends are observed for the IR process, as shown in Panel b of Figure 6 and eqs 3 and 4. The magnitude of the destabilizing effect in the conjugation by Y = $NH_2$ becomes larger in an order of Z = $CH_2$ ≪ Te < O < Se < S, while that of the stabilizing effect by Y = $NO_2$ is in an order of Z = $CH_2$ ≪ Te < Se < O ≤ S. The order is described as Z = $CH_2$ ≪ Te < Se < S: the position of O is changeable. It exists between Te and Se or between Se and S. The results support the conclusion obtained above, that is, the p(Z)−$\pi$($C_6H_4$)−p(Y) conjugations operate effectively for Z = S, Se, and Te, as well as O.

## Conclusion

The p(Z)−$\pi$($C_6H_4$)−p(Y) conjugations (Z = O, S, Se, and Te) are of high importance in terms of fundamental chemical research such as the factors to control fine structures of organic chalcogen compounds. It is inevitable to establish the contribution of the p(Z)−$\pi$(Ar) conjugation especially for Z of heavier elements, since the magnitudes of the p(Z)−$\pi$(Ar) conjugations are believed to decrease swiftly as Z becomes heavier. We established the effective p(Z)−$\pi$(Ar) conjugations for Z = S, Se, and Te, as well as Z = O, through the dynamic NMR spectroscopy of 9-(arylchalcogena)triptycenes (*p*-$YC_6H_4$ZTpc:**1** (Z = O), **2** (Z = S), **3** (Z = Se), and **4** (Z = Te)), after confirmation of the ground-state geometries by the X-ray analysis. *p*-$YC_6H_4CH_2$Tpc (**5**) was employed as the reference compound. The p(Z)−$\pi$(Ar) conjugations must operate fully in the ground states of **1**−**4**, where the *p*-$YC_6H_4$ group is placed in the bisected area between two phenyl planes of the triptycyl group with the parallel orientation. The conjugations never operate in the transition states between (**A**: **pl**) and/or the topomeric structures (**A′**: **pl′**), where the Z−$C_{Tpc}$ bond is perpendicular to the Ar plane. The activation processes must contain the loss of the p(Z)−$\pi$($C_6H_4$)−p(Y) conjugation. Temperature-dependent $^1$H NMR spectra were measured and analyzed carefully to evaluate the magnitudes of the p(Z)−$\pi$($C_6H_4$)−p(Y) conjugation for Z = S and Se having various Y.

The activation energies for the interconversion between (**A**: **pl**) and (**A′**: **pl′**) (GR: gear process) were obtained for **2** (Z = S) and **3** (Z = Se) ($\Delta G^{\ddagger}_{GR}$(**2**) and $\Delta G^{\ddagger}_{GR}$(**3**), respectively). $\Delta G^{\ddagger}_{GR}$(**3**) correlate well with $\Delta G^{\ddagger}_{GR}$(**2**): $\Delta G^{\ddagger}_{GR}$(**2**) are well analyzed by the Hammett-type dual parameters. The results demonstrate that $\Delta G^{\ddagger}_{GR}$(**2**) and $\Delta G^{\ddagger}_{GR}$(**3**) are mainly controlled by the resonance interaction through the p(Z)−$\pi$($C_6H_4$)−p(Y) conjugation. QC calculations are performed on the ground and excited states of **1**−**5**. The results clarify the effective p(Z)−$\pi$($C_6H_4$)−p(Y) conjugations for Z of heavier atoms. The established p(Z)−$\pi$($C_6H_4$)−p(Y) conjugations are very useful to understand fine structures and reactivities of organic chalcogen compounds with physical necessity.

## Experimental Section

**9-(Phenylsulfanyl)triptycene (2a).** Under a nitrogen atmosphere, to a solution of 9-bromotriptycene[33] (750 mg, 2.25 mmol) in 45 mL of benzene and 90 mL of diethyl ether at 0 °C was added 1.5 mL of *n*-BuLi (2.45 mmol, 1.63 N). After being stirred for 2 h, the supernatant liquid was removed from the fine suspension of 9-triptycyllithium by using the cannula, and 135 mL of benzene was added to the flask. A benzene solution of 1.0 equiv of phenylthiobromide was added to the 9-triptycyllithium solution. After being stirred for 10 h at 0 °C, the reaction was quenched by 4 mL of acetone. The organic layer was washed with 40 mL of 6% hydrochloric acid, 40 mL of saturated brine, 40 mL of 10% aqueous solution of sodium carbonate, 40 mL of saturated aqueous solution of sodium hydrogen carbonate, and 40 mL of saturated brine (×2) and dried over sodium sulfate. The crude product was purified by column chromatography ($SiO_2$, benzene/hexane = 1/3, v/v) and recrystallized from cyclohexane. Compound **2a** was isolated in 28% yield as colorless solid (230 mg): mp 269.0−270.0 °C; $^1$H NMR (400 MHz, $CDCl_3$/TMS) $\delta$ 5.45 (s, 1H), 6.95 (dt, *J* = 1.2, 7.6 Hz, 3H), 7.03 (dt, *J* = 1.0, 7.4 Hz, 3H), 7.06−7.17 (m, 5H), 7.42 (dd, *J* = 1.0, 7.3 Hz, 3H), 7.53 (d, *J* = 7.8 Hz, 3H); $^{13}$C NMR (100 MHz, $CDCl_3$/TMS) $\delta$ 54.0, 61.7, 123.3, 123.9, 124.5, 124.9, 125.7, 127.9, 128.3, 134.6, 143.2, 145.3. Anal. Calcd for $C_{26}H_{18}S$, C, 86.15; H, 5.01. Found: C, 85.84; H, 5.11.

**9-[*p*-(Ethoxycarbonyl)phenylsulfanyl]triptycene (2h).** Under a nitrogen atmosphere, to a solution of sodium 9-triptycylthiolate in 28 mL of DMF, prepared from 9-triptycylthiol (**6**)[34] (407 mg, 1.42 mmol) and sodium hydride (58 mg, 1.51 mmol), were added *p*-(ethoxycarbonyl)iodobenzene (390 mg, 1.41 mmol) and copper(I) iodide (27 mg, 1.38 mmol) at 70 °C. The mixture was stirred for 38 h at 110−115 °C and then poured into ice-cold water. Then, 2 mL of 36% hydrochloric acid was added. The precipitate was separated by suction filtration and extracted with 150 mL of benzene. The organic layer was washed with 25 mL of a 28% aqueous solution of ammonia (×2) and 30 mL of water (×2) and dried over sodium sulfate. The crude product was purified by column chromatography ($SiO_2$, benzene/hexane = 3/1, v/v) and GPC and recrystallized from dichloromethane and *n*-hexane. Compound **2h** was isolated in 47% yield as a colorless solid (286 mg): mp 219.0−220.0 °C; $^1$H NMR (400 MHz, $CDCl_3$/TMS) $\delta$ 1.34 (t, *J* = 7.1 Hz, 3H), 4.33 (q, *J* = 7.1 Hz, 2H), 5.46 (s, 1H), 6.95 (dt, *J* = 1.1, 7.6 Hz, 3H), 7.05 (dt, *J* = 1.0, 7.4 Hz, 3H), 7.18 (d, *J* = 8.5 Hz, 2H), 7.44 (dd, *J* = 0.9, 7.3 Hz, 3H), 7.47 (d, *J* = 7.6 Hz, 3H), 7.82 (d, *J* = 8.7 Hz, 2H); $^{13}$C NMR (100 MHz, $CDCl_3$/TMS) $\delta$ 14.3, 53.9, 60.8, 61.9, 123.5, 123.6, 124.9, 125.8, 126.6,

(31) The frequency analysis on the optimized structures of **2a** (**B**: **pd**) and **2a** (**A**: **pd**) (Y = H: $C_s$ symmetry) gave only one negative frequency with the rest positive frequencies. The results show that (**B**: **pd**) and (**A**: **pd**) must be the transition states for the GR and IR processes, respectively, in **2a**. As an analogy, (**B**: **pd**) and (**A**: **pd**) are identified as the transition states for the GR and IR processes in **1**−**5**, respectively.

(32) The reason must be the steric repulsion between the C−H bonds of the $CH_2$ group and the C9−$C_{Ar}$ bonds at the TS of the (**B**: **pd**) type in **5a**. See ref 19.

(33) Bartlett, P. D.; Cohen, S. G.; Cotman, J. D., Jr.; Kornblum, N.; Landry, J. R.; Lewis, E. S. *J. Am. Chem. Soc.* **1950**, *72*, 1003–1004.

(34) Kawada, Y.; Ishikawa, J.; Yamazaki, H.; Koga, G.; Murata, S.; Iwamura, H. *Tetrahedron Lett.* **1987**, *28*, 445–448.

127.6, 129.2, 141.1, 142.6, 145.2, 166.2. Anal. Calcd for $C_{29}H_{22}O_2S$, C, 80.15; H, 5.10. Found: C, 80.13; H, 5.37.

**9-Triptycylthiol (6).** Compound **6** was prepared in 37% yield as colorless solid according to the same procedure as described in the literature:[34] mp 262.5−263.5 °C (from cyclohexane); $^1$H NMR (400 MHz, $CDCl_3$/TMS) $\delta$ 2.41 (s, 1H), 5.43 (s, 1H), 7.02−7.09 (m, 6H), 7.38−7.42 (m, 3H), 7.68−7.72 (m, 3H); $^{13}$C NMR (100 MHz, $CDCl_3$/TMS) $\delta$ 53.7, 58.9, 121.8, 123.2, 125.0, 125.7, 144.9, 145.5. Anal. Calcd for $C_{20}H_{14}S$, C, 83.88; H, 4.93. Found: C, 83.88; H, 4.75.

**9-(*p*-Nitrophenylsulfanyl)triptycene (2j).** Under a nitrogen atmosphere, to a solution of sodium 9-triptycylthiolate in 2 mL of DMF, prepared from **6**[34] (107 mg, 0.375 mmol) and sodium hydride (14 mg, 0.375 mmol), was added *p*-nitroiodobenzene (100 mg, 0.402 mmol) at 70 °C. After being stirred for 3 h at 70 °C, the reaction was quenched by 10 mL of water. Then, 10 mL of 6% hydrochloric acid and 40 mL of benzene were added. The organic layer was separated and then washed with 10 mL of saturated brine, 10 mL of 10% aqueous solution of sodium carbonate, 10 mL of saturated aqueous solution of sodium hydrogen carbonate, and 10 mL of saturated brine (×2) and dried over potassium carbonate. The crude product was purified by column chromatography ($SiO_2$, benzene/hexane = 1/1, v/v) and recrystallized from cyclohexane. Compound **2j** was isolated in 74% yield as yellow leaflets (113 mg): mp 296.5−297.5 °C; $^1$H NMR (400 MHz, $CDCl_3$/TMS) $\delta$ 5.49 (s, 1H), 6.97 (dt, $J$ = 1.2, 7.6 Hz, 3H), 7.07 (dt, $J$ = 0.9, 7.3 Hz, 3H), 7.25 (d, $J$ = 7.8 Hz, 2H), 7.42 (d, $J$ = 7.8 Hz, 3H), 7.47 (d, $J$ = 7.3 Hz, 3H), 8.01 (d, $J$ = 9.2 Hz, 2H); $^{13}$C NMR (100 MHz, $CDCl_3$/TMS) $\delta$ 53.9, 62.3, 123.3, 123.4, 123.7, 125.0, 126.2, 128.2, 142.2, 144.6, 144.8, 145.2. Anal. Calcd for $C_{26}H_{17}NO_2S$, C, 76.64; H, 4.21; N, 3.44. Found: C, 76.80; H, 4.17; N, 3.44.

Experimental procedure and analytical data for **1a**,**j**, **2b**−**g**,**i**, and **5a** are given in the Supporting Information.

**Analysis of $^1$H DNMR.** $^1$H DNMR spectra for **2** and **3** were measured in $CD_2Cl_2$ solutions (0.04 M) at variable temperature on a 400 MHz spectrometer. The temperature-dependent spectra of the aromatic protons of **2f**−**j** and **3g**−**j** were analyzed using an NMR simulation program, *gNMR*[25] (see Figure 2, for example). The free energies of activation ($\Delta G^{\ddagger}$ (kJ mol$^{-1}$)) at the coalescence temperature ($T_c$ (K)) were obatained by eq 5.[26] The chemical shift differences ($\Delta\nu$ (Hz)) were obtained as described above.

$$\Delta G^{\ddagger} = RT_c \times (22.96 + \ln(T_c/\Delta\nu)) \quad (R{:}8.31447\ \text{J K}^{-1}, \text{gas constant}) \quad (5)$$

**X-ray Structural Determination of 1a,j, 2a,j, and 5a.** Single crystals of **1a**,**j** and **2a**,**j** were obtained from solutions of *n*-hexane/dichloromethane (2/1, v/v) after slow evaporation of the solvent at room temperature, **5a** from a solution of *n*-hexane/ethyl acetate (3/2, v/v). Diffraction data were collected on a CCD diffractometer equipped with a graphite-monochromated Mo Kα radiation source ($\lambda$ = 0.71070 Å) at 233 K. The structures were solved by direct methods (SHELXS-97)[35] and refined by full-matrix least-squares methods on $F^2$ for all reflections (SHELXL-97)[36] with all non-hydrogen atoms anisotropic and all hydrogen atoms isotropic. CCDC-722553 for **1a**, CCDC-722554 for **1j**, CCDC-722555 for **2a**, CCDC-722556 for **2j**, and CCDC-722557 for **5a** contain the supplementary crystallographic data for this paper. These data can be obtained free of charge from the Cambridge Crystallographic Data Centre via http://www.ccdc.cam.ac.uk/data request/cif.

**QC Calculations.** QC calculations were performed on (**A**: **pl**), (**A**: **pd**), and (**B**: **pd**) of **1**−**5** having Y = H (**a**), $NH_2$ (**1b′**), and $NO_2$ (**j**) using the Gaussian 03 program.[28] The MP2[29] level was applied for the calculations. The 6-31G(d) basis sets were employed for H, C, and N of **1**−**5**. The 6-311+G(d) basis sets were employed for O in **1** and the 6-31G(d) basis sets for O in **2**−**5**. The 6-311+G(d) basis sets were employed for S and Se in **2** and **3** and the reported basis sets[30] of the (7433111/743111/7411/2 + 1s1p1d1f) type for Te in **4**.

**Acknowledgment.** This work was partially supported by Grants-in-Aid for Scientific Research (Nos. 16550038 and 19550041) from the Ministry of Education, Culture, Sports, Science, and Technology, Japan. The support of the Kitasato University Research Grant for Young Researchers (to M.M.) is also acknowledged.

**Supporting Information Available:** ORTEP drawing of **1a**,**j**, **2j**, and **5a**, selected interatomic distances, angles, and torsional angles of **1a**,**j**, **2a**,**j**, and **5a**, together with those of **3a**, observed $^1$H NMR spectra due to the aromatic proton region of **2** and **3** in $CD_2Cl_2$ at various temperatures, together with the calculated spectra with the best-fit rate constants for the aromatic protons for the GR and/or IR processes, experimental procedure for **1a**,**j**, **2b**−**g**,**i**, **5a**, and **7**, analytical data for **1j**, **2a**−**j**, **6**, and **7**, and X-ray crystallographic files of **1a**,**j**, **2a**,**j**, and **5a** (CIF). Structures and energies for **1**−**5** with Y = H (**a**), $NH_2$ (**1b′**), and $NO_2$ (**j**) in (**A**: **pl**), (**A**: **pd**), and (**B**: **pd**), optimized with the MP2 method. This material is available free of charge via the Internet at http://pubs.acs.org.

JO900488R

(35) Sheldrick, G. M. *SHELXS-97, Program for Crystal Structure Solution*; Universität Göttingen: Göttingen, 1997.

(36) Sheldrick, G. M. *SHELXL-97, Program for Crystal Structure Refinement*; Universität Göttingen: Göttingen, 1997.